Journal of
Composites Science

MDPI

Article

Characterization of *Posidonia oceanica* Fibers High-Density Polyethylene Composites: Reinforcing Potential and Effect of Coupling Agent

Manel Haddar [1], Ahmed Elloumi [1], Cheldly Bradai [1] and Ahmed Koubaa [2,*]

[1] École Nationale d'Ingénieurs de Sfax (ENIS), Université de Sfax, Sfax 3038, Tunisia; haddar.manel26@gmail.com (M.H.); loumiahmed@gmail.com (A.E.); chedly.bradai@enis.tn (C.B.)
[2] Institut de Recherche sur les Forêts, Université du Québec en Abitibi-Témiscamingue (UQAT), 445, Boulevard de l'Université, Rouyn-Noranda, QC J9X 5E4, Canada
* Correspondence: ahmed.koubaa@uqat.ca

Abstract: This study investigated the influence of fiber loading and maleated polyethylene (MAPE) coupling agent on the structural, thermal, mechanical, morphological properties, and torque rheology of high-density polyethylene (HDPE) reinforced with *Posidonia oceanica* fiber (POF) composites. HDPE/POF composites, both with and without MAPE, were manufactured using a two-step process: composite pellets extrusion, followed by test samples injection molding with various POF loadings (0, 20, 30, and 40 wt%). HDPE/POF composites reinforced with higher loading of POF (40 wt%) exhibit superior stiffness, better crystallinity, and higher stabilized torque and mechanical energy (E_m) compared to other composite formulations. Therefore, varying the POF loading leads to extrusion and injection processing variations. Furthermore, the coupling agent significantly enhances the tensile strength, ductility, impact strength, crystallinity, stabilized torque, and E_m of the HDPE/POF composite. This improvement is due to the enhanced interfacial adhesion between the POF and the HDPE matrix with the addition of the MAPE, as supported by the Scanning Electron Microscopy (SEM) micrographs.

Keywords: *Posidonia oceanica* fibers (POFs); high-density polyethylene (HDPE); HDEP/POF composite; thermal properties; mechanical properties; torque rheology

Citation: Haddar, M.; Elloumi, A.; Bradai, C.; Koubaa, A. Characterization of *Posidonia oceanica* Fibers High- Density Polyethylene Composites: Reinforcing Potential and Effect of Coupling Agent. *J. Compos. Sci.* **2024**, *8*, 236. https://doi.org/10.3390/jcs8070236

Academic Editor: Francesco Tornabene

Received: 19 March 2024
Revised: 1 May 2024
Accepted: 14 June 2024
Published: 24 June 2024

1. Introduction

In recent years, increasing interest has been in incorporating lignocellulosic fibers to reinforce composite materials. This growing interest can be attributed to their numerous advantages, including their sustainable nature, availability, renewability, biodegradability, cost-effectiveness, low density, exceptional in-service properties, and especially their recyclability compared to glass or carbon synthetic fibers [1–5].

Substituting synthetic fibers with lignocellulosic fibers is a prominent strategy for enhancing the composites' sustainability because the energy consumption related to natural fiber production is about half that of synthetic fiber, and the generated carbon dioxide emissions are much lower [6]. Natural fibers including flax [7,8], kenaf [9], alfa [10], bamboo [11,12], oil palm [13], sugar palm [14–16], jute [17], sisal [18], hemp [19], etc., have been utilized as reinforcements in composites materials. Composites reinforced with natural fiber or biocomposites find applications in the automotive, construction, aerospace, and marine sectors [5,20–22]. Cars' interior parts are among the composites' popular uses because of their good tensile strength and reduced flammability [23,24]. Several thermoset and thermoplastic polymers serve as matrices for natural fibers in composite materials. Compared to thermoset polymers, thermoplastic polymers are commonly used matrices in natural fibers' composites because of their advantages, including cost-effective processing, availability, and better flexibility and processing temperatures, generally below 200 °C, which prevent

the natural fibers from thermal degradation [4,21,25]. Moreover, the growing focus on environmental concerns has increased interest among researchers in thermoplastic-based composites, thanks to their potential for recycling and incineration [21,26,27]. Recently, many authors have utilized a variety of thermoplastic polymers, such as polyethylene, polypropylene, polyvinyl chloride, polystyrene, and polyamide 6 (PA6), as matrices to develop novel natural fibers-reinforced composite materials [4,21]. Thermoplastic reinforced with lignocellulosic fibers could be manufactured by either extrusion or mold-injection processes [28]. However, lignocellulosic fibers and the thermoplastic polymers are incompatible due to the fibers' hygroscopicity and polarity and the polymers' non-polarity and hydrophobicity. Furthermore, fibers' hemicellulose, lignin, pectin, and waxes create smooth surfaces, resulting in poor interlocking and adhesion in the fiber–polymer interface [28,29]. Therefore, numerous investigators have employed surface treatment methods, including physical and chemical treatments, or used silanes or maleic anhydride as coupling agents to enhance the polymer–fiber interfacial adhesion [6,28–30]. Zainal et al. [31] studied the effect of alkaline and silane treatments on tensile, thermal, chemical, and morphological properties of a PP/recycled acrylonitrile butadiene rubber (NBRr)/sugarcane bagasse (SCB) powder composite. They indicated that chemical treatment of the SCB fiber improves the thermal stability and tensile properties of the PP/NBRr/SCB composites. They also reported that the silane-treated composites generated better results regarding the evaluated properties. Madhavi et al. [32] studied the influence of a coupling agent (Maleic Anhydride Polypropylene (MAPP)) on the thermal, structural, morphological, and mechanical properties of bamboo fiber-reinforced polypropylene composites. They showed that the Bamboo–PP composite coupled with MAPP exhibited higher mechanical strength (tensile and flexural), improved thermal stability, and lower water absorption than the Bamboo–PP composite without MAPP. SEM observations also confirmed the good interfacial adhesion between PP and bamboo fiber when using a coupling agent. Furthermore, Li [33] found that adding a coupling agent (MAPE) enhanced the flexural and tensile properties of wood/HDPE composites and improved the interfacial adhesion, as evidenced by the SEM micrographs. Hachaichi et al. [34] recently studied the effects of alkali surface modification and a compatibilizer agent on HDPE's mechanical behavior and microstructure reinforced with date palm fiber (DPF) biocomposites. The results indicated that incorporating 30 wt% of DPF treated with NaOH and KMnO4 (DPF2) in the HDPE biocomposite improved the mechanical and morphological properties. The highest Young's modulus was obtained when 10 wt% of maleic anhydride grafted high-density polyethylene (HDPE-g-MA) was used as a compatibilizer agent in the 30 wt% DPF2/HDPE biocomposites.

This study aims to utilize the abundant and renewable lignocellulosic *Posidonia oceanica* fibers (POFs) as a potential reinforcement agent for composites based on a thermoplastic HDPE matrix. It aims to investigate the impact of POF loadings (0, 20, 30, and 40 wt%) and a coupling agent (3 wt% MAPE) on the structural, thermal, mechanical, and morphological properties as well as torque rheology of the developed HDPE/POF composites.

2. Materials and Methods

2.1. Materials and Preparation of POF/HDPE Composites

The *Posidonia oceanica* fibers (POFs) used in this study were collected and prepared in previous work [25]. The fibers' chemical composition, morphology, structure, and thermal stability were presented in a previous report [25]. It is important to note that the POF has an average diameter of 100 µm. POFs were used as reinforcement agents for the composite materials made with a thermoplastic matrix.

A sawmill in La Sarre, Quebec, Canada supplied the black spruce wood fibers (WFBS) utilized in this work. Before preparing the composite, the fibers underwent air-drying until they reached a dry basis moisture content of approximately 10%. Subsequently, they were milled using a Wiley Laboratory Mill Model 4 equipped with a 2 mm opening sieve and then sieved using a Ro-tap Laboratory Sieve Shaker. The fraction with openings ranging

from 150 to 710 µm was retained for the composite elaboration. The fibers underwent oven drying at 80 °C as a final step until they reached a dry basis moisture content of around 3%.

POFs reinforced with high-density polyethylene (HDPE) composites were produced in a two-step process: pellet extrusion followed by test samples injection molding. A counter-rotating intermeshing conical twin-screw extruder (Thermo Scientific HAAKE PolyLab OS Rheodrive 7 with Rheomex OS extruding module, Karlsruhe, Germany) was utilized to mix POF with HDPE (SCLAIR®2815, Nova Chemical (density of 0.952 g/cm^3 and melt flow index of 69 g/10 min at 190 °C)) and 3 wt% of maleated polyethylene (MAPE, Fusabond E226, DuPont (melt flow index of 1.75 g/10 min at 190 °C)) to produce various composite formulations (Table 1). The average screw speed was 50 rpm, and the temperature of the barrels and die was 170 °C. After cooling the extrudate in a water bath, it was ground into pellets of approximately 3 mm length. Subsequently, the pellets were oven-dried at 80 °C overnight to achieve a dry basis moisture content of about 3%. The pellets were then molded for tensile and impact specimens using an Arburg 370A (600 kN) injection molding machine (Lossburg, Germany). Injection molding parameters were 30 °C mold temperature, 140 MPa injection pressure, 2 s injection time, 70 MPa holding pressure, 11 s holding time, barrel temperature profile 190 to 170 °C, and 17 s cooling time. The obtained specimens were conditioned for a minimum of 48 h at 20 °C and 50% relative humidity until their mass stabilized.

Table 1. Formulations of the prepared composites.

Composite Formulations	HDPE Content (wt.%)	POF Content (wt.%)	MAPE Content (wt.%)
Virgin HDPE	100	0	0
HDPE/POF/MAPE (80/20/0)	80	20	0
HDPE/POF/MAPE (77/20/3)	77	20	3
HDPE/POF/MAPE (70/30/0)	70	30	0
HDPE/POF/MAPE (67/30/3)	67	30	3
HDPE/POF/MAPE (60/40/0)	60	40	0
HDPE/POF/MAPE (57/40/3)	57	40	3

2.2. Characterization

The HDPE and its POF composites were analyzed using attenuated total reflection Fourier Transform Infrared Spectroscopy (ATR-FTIR) with a Nicolet OMNIC 560 Fourier transform spectrometer (Thermofisher, Wilmington, NC, USA). Composite specimens were scanned over the 4000 to 400 cm^{-1} range with a resolution of 4 cm^{-1}.

The thermal stability of HDPE and POF composites was studied by thermogravimetric analysis (TGA) and differential scanning calorimetry (DSC). Thermogravimetric analysis was performed on a TGA Q50 analyzer (TA Instruments, New Castle, DE, USA). Composite specimens weighing 10.5 and 11.5 mg were heated from 25 to 800 °C at a rate of 10 °C/min in a nitrogen atmosphere with a flow rate of 60 mL/min. The DSC Q20 equipment was utilized to investigate the crystallization properties. The thermal program detailed by Bouafif et al. [35] was adopted to determine the melting behavior and crystallization rate. The degree of crystallinity χ_c (%) for all composite formulations was determined using Equation (1):

$$\chi_c\ (\%) = \Delta H_m \times 100/\Delta H^{\circ}_{100\%\ \text{Crystallinity}} \times W_f \quad (1)$$

where ΔH_m and $\Delta H^{\circ}{}_{100\%\ \text{crystallinity}}$ are the composite specimens' melting enthalpy determined by the DSC curve and the enthalpy of 100% crystalline HDPE = 288 J/g [36], respectively. W_f is the mass fraction of HDPE in the composite. All thermal tests were conducted at least twice for each sample.

Tensile tests were conducted according to ASTM D 638 [37] using specimen Type IV and a crosshead speed of 5 mm/min. Un-notched impact tests were conducted according to ASTM D 4812 [38] using a 2.75 J pendulum. At least seven samples were tested for each

composite. The fractured surfaces of the tensile composite specimens were analyzed using Scanning Electron Microscopy (SEM) (Hitachi S-3500N).(Hitachi High-Tech, Tokyo, Japan).

The composites' torque rheology properties were measured using a torque rheometer from HAAKE, Germany. The POF and HDPE pellets were mixed in the Haake mixer with a consistent fill level of 65% for 12 min while maintaining a rotor speed of 50 rotations per minute (RPM) at a temperature of 170 °C.

3. Results

3.1. Surface Chemistry

FTIR spectroscopy was employed to determine if chemical reactions occurred or if any new functional groups appeared in the Virgin HDPE after introducing the POF or adding the MAPE. FTIR spectra of the Virgin HDPE and HDPE/POF composites (with and without MAPE) are depicted in Figure 1. The peaks at 2916, 2849, 1462, and 717 cm^{-1} are attributed to the methylene groups present in HDPE [39,40]. The introduction of POF into the HDPE matrix results in the appearance of a broad band between 3600 and 3200 cm^{-1} in the FTIR spectra of HDPE/POF composites, which is assigned to the stretching vibration of the OH groups of the fibers [39,41,42]. It should be noted that the peaks at 2916 and 2849 cm^{-1} shift to a lower range as the POF content increases in the composites. This shift can be attributed to the interaction between the chains of HDPE and those of POF [43]. Furthermore, we detected two new absorption peaks at 1597 and 1032 cm^{-1} in the FTIR spectra by introducing POF into the HDPE matrix for all HDPE/POF composites. The peak at 1597 cm^{-1} is assigned to the C=C stretching vibration of the substituted aromatic ring in lignin [44,45], and the peak at 1032 cm^{-1} is attributed to the C-OH stretching vibration of the cellulose [42,44]. As shown in Figure 1, adding a coupling agent makes it possible to decrease the hydrophilicity of the POF by reducing the intensity of hydroxyl groups in the range of 3600–3200 cm^{-1}. Lower hydroxyl group intensity results from a reaction with the MAPE [46].

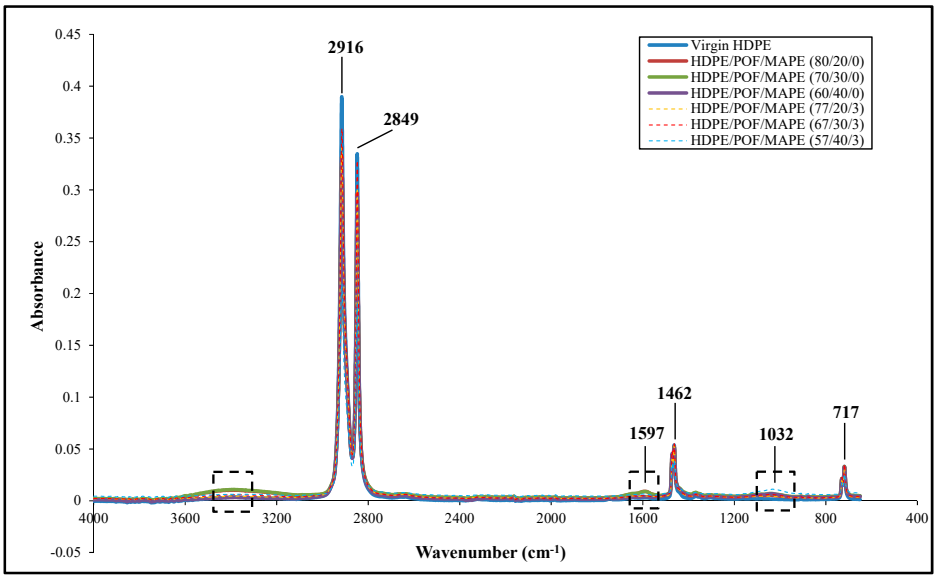

Figure 1. FTIR spectra of Virgin HDPE and HDPE/POF composites (with and without 3% MAPE).

3.2. Thermal Stability

3.2.1. Thermogravimetric Analysis

Figure 2a,b show the weight losses (TGA) and time derivatives of the weight (DTG) curves of the HDPE polymer and its POF composites (with and without coupling agent), respectively. Results show that the weight loss of Virgin HDPE occurred in a one-step degradation process from 320 to 500 °C (Figure 2a). The presence of only one peak at 460 °C on the DTG curve (Figure 2b) confirms this result. This thermal behavior can be

associated with the homogeneous structure of the thermoplastic HDPE, which decomposes into ethylene monomers. Previous studies [47,48] reported similar findings. However, the composites' thermal degradation occurred in two degradation steps (Figure 2a). The first step, from 220 to 350 °C, is related to the decomposition of hemicelluloses and cellulose fibers, and this was confirmed by the presence of two peaks on the DTG curve (Figure 2b). The second degradation step, from 350 to 520 °C, is attributed to the decomposition of the HDPE, which is in good agreement with previous findings [48,49] for HDPE/wood composites and LDPE/palm composites, respectively. Above 520 °C, it is important to note that increasing the percentage of POF from 20 to 40% led to increased residual amount, primarily attributed to the increase in ash content. Similar findings were reported by Torres-Tello et al. [50] for a green composite based on poly(hydroxybutyrate-co-hydroxyvalerate (P(HB-HV)) reinforced with agave fiber. They found that the higher fiber ratio increased the formation of residual amount due to the presence of ashes.

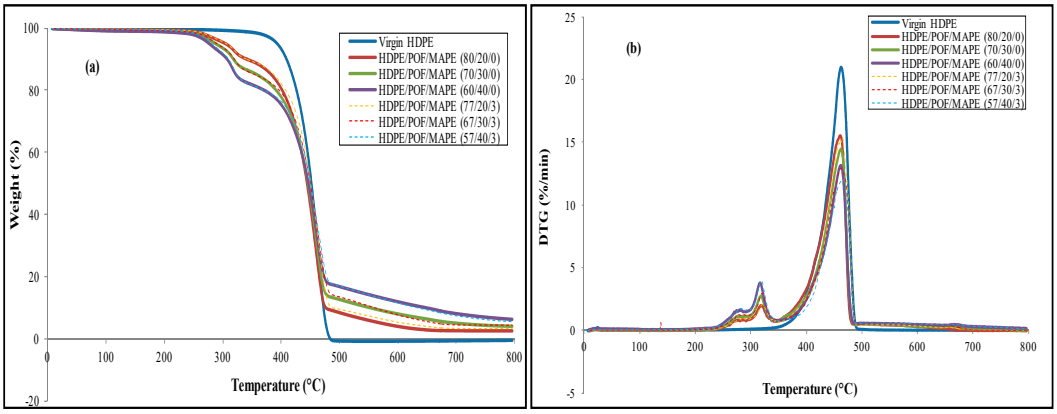

Figure 2. TGA (**a**) and DTG (**b**) curves of Virgin HDPE and HDPE/POF composites (with and without 3% MAPE).

Table 2 displays the initial degradation temperature (T_{onset} (°C)), the weight loss (%), and the maximum degradation temperature (DTG_{max} (°C)) for Virgin HDPE and HDPE/POF composites (with and without 3% MAPE), obtained from TGA and DTG curves.

Table 2. Thermal properties of the Virgin HDPE and HDPE/POF composites obtained by TGA and DTG curves.

Samples	T_{onset} (°C) *	Degradation Step	Temperature Range (°C)	Weight Loss (%)	DTG_{max} (°C)
Virgin HDPE	388.8 ± 6.7	First Second	- 320–500	- 99.8 ± 0.6	- 460.5 ± 2.7
HDPE/POF/MAPE (80/20/0)	304.8 ± 1.1	First Second	220–350 350–520	9.5 ± 0.1 82.1 ± 0.0	318.3 ± 0.5 457.8 ± 1.1
HDPE/POF/MAPE (70/30/0)	286.0 ± 4.2	First Second	220–350 350–520	12.6 ± 0.2 73.7 ± 0.8	318.3 ± 0.5 463.1 ± 1.1
HDPE/POF/MAPE (60/40/0)	278.5 ± 0.7	First Second	220–350 350–520	16.0 ± 0.1 66.1 ± 0.1	317.2 ± 1.1 462.0 ± 0.5

* T_{onset} is defined as 5% weight loss.

Based on the results of thermal properties summarized in Table 2, it was noticed that the addition of POF to the HDPE matrix decreased the T_{onset} of all HDPE/POF composites compared to Virgin HDPE (from 388.8 to 278.5 °C for Virgin HDPE and HDPE/POF/MAPE (60/40/0) composite, respectively). Therefore, adding POF reduced the thermal stability of the HDPE/POF composites. Additionally, lignocellulosic fibers (POF) display lower

thermal stability compared to the HDPE matrix, which is in good agreement with previous findings [47,51] for thermoplastic polymers reinforced with natural fibers. In the first degradation step, the reduction in thermal stability of the HDPE/POF composites with the increase in percentage of POF was confirmed by the decrease in DTG_{max} (from 318.3 to 317.2 °C for composites reinforced with 20 and 40% of POF, respectively) and the increase in weight loss (from 9.5 to 16% for composites reinforced with 20 and 40% of POF, respectively) (see Table 2). Similar results were found by Yang et al. [52] for LDPE reinforced with rice husk flour (RHF) composites. In the second degradation step, it can be seen from Table 2 that the DTG_{max} is shifted from 460.5 up to 462.0 °C for the Virgin HDPE and HDPE/POF composite reinforced with 40% POF, respectively. This increase can be attributed to the synergistic effect that delays the degradation temperature of HDPE/POF composites, and this is related to the existence of the natural phenolic compounds in *Posidonia oceanica* [53].

From the TGA and DTG curves (Figure 2a,b), we observe that adding 3% MAPE has no effect on the thermal behavior of HDPE/POF composites, and the intensity of the peaks remains unchanged.

3.2.2. Differential Scanning Calorimetry (DSC)

DSC melting curves of the Virgin HDPE and HDPE/POF composites (with and without 3% MAPE) are shown in Figure 3, and the melting temperature (T_m), enthalpy of melting (ΔH_m), and percentage of crystallinity (χ_c) are presented in Table 3. From Figure 3 and Table 3, the T_m values of the HDPE/POF composites (with and without coupling agent) were similar to those of the Virgin HDPE, and no correlation with the POF content was established. Similar results are found by Borja et al. [54] for PP/cellulose composite. As observed in Table 3, POF increased the χ_c from 67.9% for HDPE to 70% for the HDPE/POF composite reinforced with 40 wt% POF. This result can be attributed to the nucleating capacity of the POF in facilitating the crystallization process of the HDPE matrix, as reported in previous works [54–56] for PP/sisal fiber composite, PP/pulp fiber (cellulose I) composite, and PP/date palm tree fiber composite, respectively. Incorporating the cellulose filler into the matrix takes place in the amorphous zone of the material, and the surface of the filler acts as a nucleation site, which modifies the crystallization kinetics of the semi-crystalline thermoplastic polymer. By examining the crystallinity values of uncompatibilized and compatibilized HDPE/POF composites presented in Table 3, it is evident that adding 3 wt% MAPE improved the crystallinity of the materials. This improvement in crystallinity results from the nucleating effect of MAPE, which promotes the formation of more crystals compared to the HDPE/POF composite without MAPE, in agreement with previous findings on the HDPE/hemp composite [51].

Table 3. Crystallization and melting characteristics of the HDPE polymer and the HDPE/POF composites (with and without coupling agent).

Sample	T_m (°C)	ΔH_m (J/g)	χ_c (%)
Virgin HDPE Polymer	128.7 ± 0.1	195.7 ± 3.1	67.9 ± 1.1
HDPE/POF/MAPE (80/20/0)	128.8 ± 0.1	151.2 ± 0.4	65.6 ± 0.2
HDPE/POF/MAPE (70/30/0)	128.6 ± 0.0	137.7 ± 0.1	68.3 ± 0.1
HDPE/POF/MAPE (60/40/0)	128.5 ± 0.1	120.9 ± 0.3	70 ± 0.2
HDPE/POF/MAPE (77/20/3)	128.7 ± 0.3	154.65 ± 0.1	69.7 ± 0.0
HDPE/POF/MAPE (67/30/3)	128 ± 0.0	134.15 ± 0.5	69.5 ± 0.3
HDPE/POF/MAPE (57/40/3)	128.2 ± 0.0	118.9 ± 0.4	72.4 ± 0.3

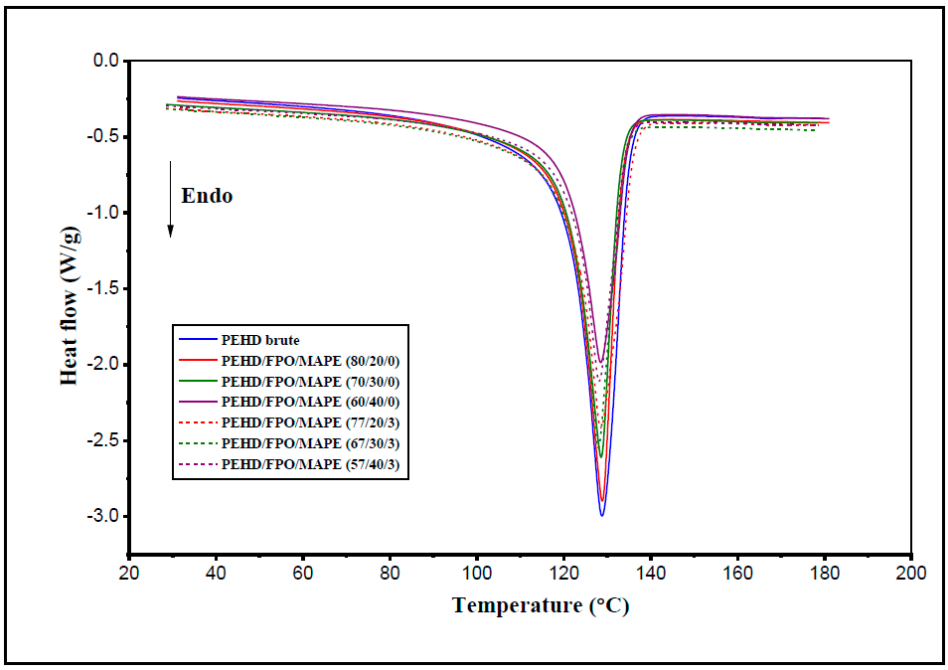

Figure 3. DSC curves of the second heating cycle of Virgin HDPE and HDPE/POF composites (with and without 3% MAPE).

3.3. Mechanical Properties of HDPE/POF Composites

Figure 4 illustrates the stress–strain curves obtained from the tensile tests for HDPE/POF composites reinforced with different POF rates (with and without coupling agent). The maximum stress was obtained with HDPE/POF composite reinforced with 40 wt% POF, which also showed lower strain compared to HDPE/POF composites reinforced with 20 and 30 wt% POF (see Figure 4). Further, adding the coupling agent exhibited an enhancement in the ductility of the materials, and this was revealed by the increase in the strain of compatibilized HDPE/POF composites compared to uncompatibilized HDPE/POF composites (see Figure 4). Figure 5 shows the influence of the POF rate and the coupling agent on the composites' tensile modulus of elasticity (E), strength (TS), and elongation at break (ε_r). Compared to Virgin HDPE, the introduction of POF enhanced the composite rigidity. Specifically, incorporating 20, 30, and 40 wt% of POF increased Young's modulus by about 53.8, 65.5, and 74.2%, respectively (Figure 5a). This result confirms the reinforcing effect of POF on the polymer, in agreement with the previous findings [3,25,53,57,58] for composites based on thermoplastic or thermoset matrices reinforced with POF. In conclusion, HDPE/POF composites reinforced with a higher percentage of POF (40 wt%) exhibit greater rigidity and better crystallinity than other composite formulations.

Figure 5a shows that the coupling agent did not affect the Young's modulus of HDPE/POF composites. In addition, the TS appears to be either conserved with interesting values close to 15–17 MPa for HAPE/POF composites containing 0, 20, and 30 wt% POF and slightly improved by about 2.35% for the HDPE/POF composite reinforced with 40 wt% POF compared to Virgin HDPE (Figure 5b). The addition of MAPE increased the TS with increasing POF content in the HDPE/POF composites (Figure 5b). Thus, the coupling agent in HDPE/POF composites containing 20, 30, and 40 wt% of POF increased the TS by about 23.44, 33.21, and 40.53%, respectively, compared to HDPE/POF composites without MAPE. This improvement in TS is attributed to the enhanced interfacial adhesion between the POF and HDPE matrix resulting from the addition of the coupling agent, as evidenced by the SEM micrographs reported in our previous work [25]. However, the ε_r of the HDPE/POF composites decreased with increasing POF content from 5.01 to 2.02% for composites containing 20 and 40 wt% POF, respectively (Figure 5c). This behavior is attributed to the stiffening effect of the lignocellulosic POF, resulting in brittle fracture in

the HDPE/POF composites. Adding the coupling agent led to a higher elongation at break compared to the composites without a coupling agent, resulting in increased ductility of the material (Figure 5c).

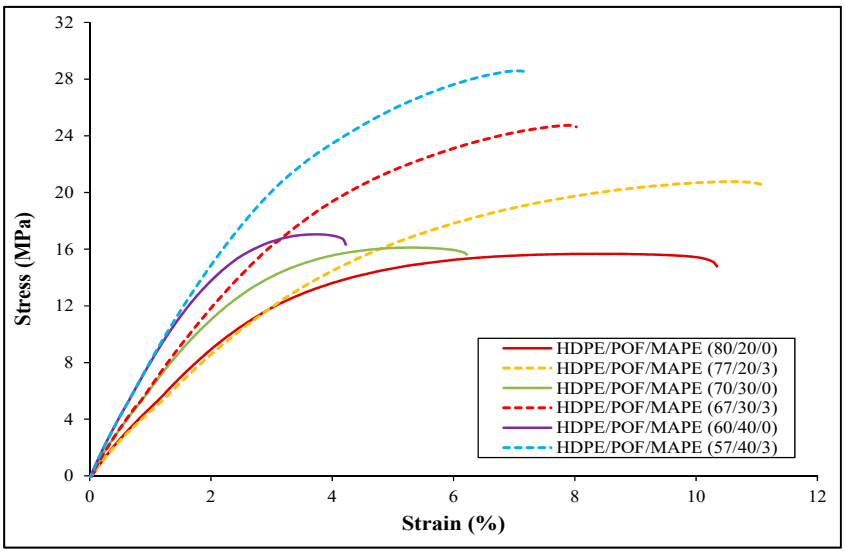

Figure 4. Stress–strain curves for HDPE/POF composites reinforced with different percentages of POF (with and without 3% MAPE).

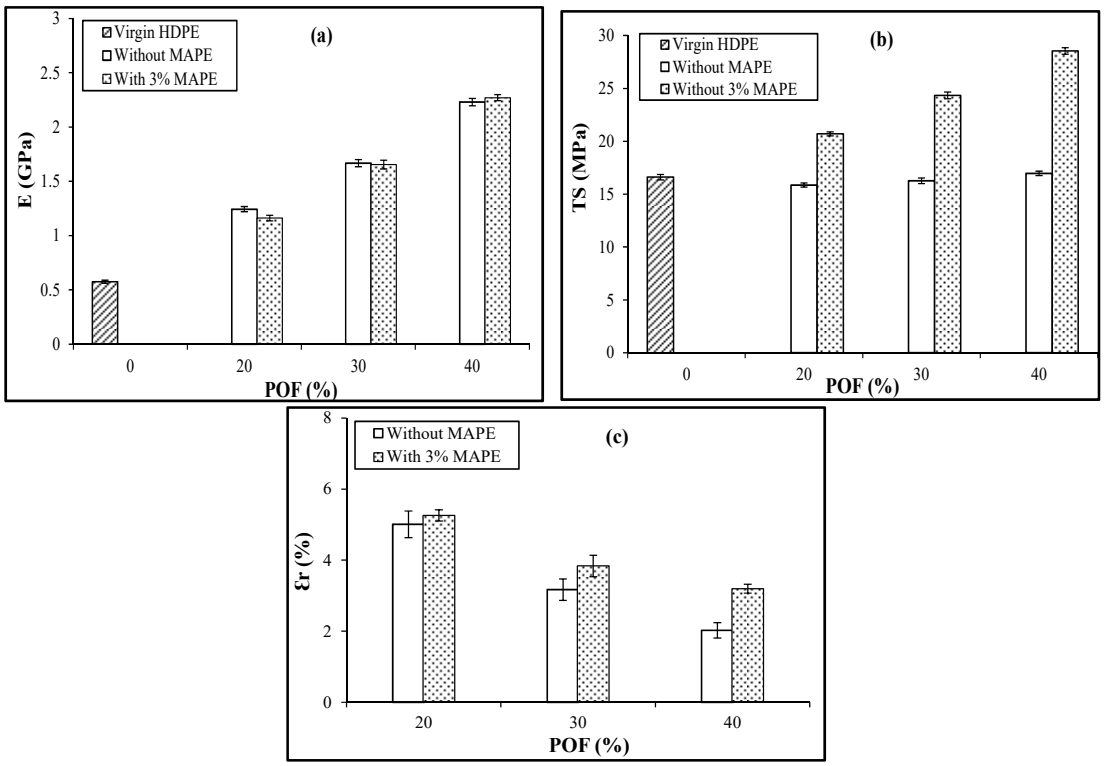

Figure 5. Bar plot of tensile tests of HDPE/POF composites reinforced with different POF rates (with and without 3% MAPE): (**a**) modulus of elasticity (E), (**b**) tensile strength (TS), and (**c**) elongation at break (ε_r).

Figure 6 depicts the SEM micrographs of the fractured tensile surface of HDPE/POF composites reinforced with 30 wt% of POF, both with and without a coupling agent. It is clear that adding MAPE improves fiber–matrix adhesion and restricts fiber debonding, as

observed in Figure 6a for the HDPE/POF composite without MAPE. Moreover, the SEM micrograph demonstrates that the addition of the MAPE leads to better impregnation of POFs into the HDPE polymer matrix (Figure 6b), confirming the ductile deformation of the HDPE/POF composite with 3 wt% MAPE (Figure 5c).

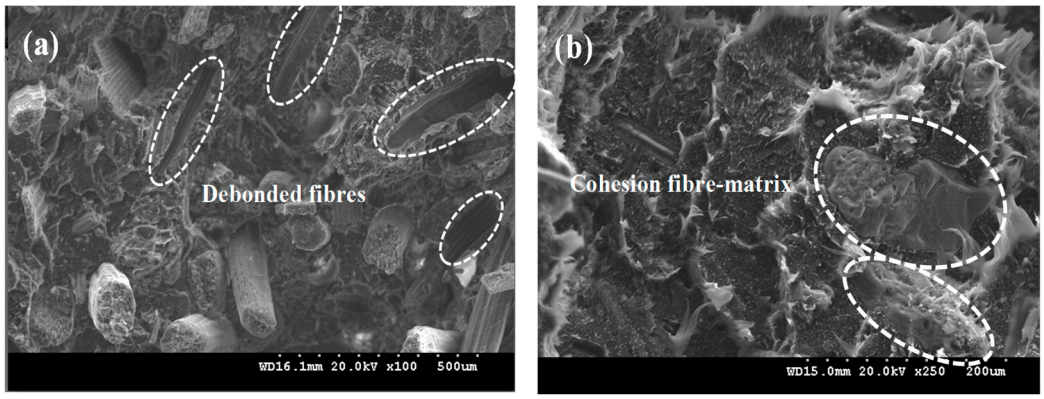

Figure 6. SEM micrographs of the HDPE/POF composite's fracture surface contain 30% POF (**a**) without MAPE and (**b**) with 3% MAPE.

Figure 7 illustrates the impact energy (aK) of the HDPE/POF composites (with and without MAPE). A significant reduction in aK is observed as the POF content increases from 20 to 40 wt%. Increasing the POF content increases the stress concentration due to poor fiber–matrix interfacial adhesion [59]. Similar results were also reported by Naghmouchi et al. [60], who found that the impact energy of polypropylene reinforced with an olive stone flour (OSF) composite decreased as the OSF content increased. Figure 7 shows that a 3 wt% coupling agent in the HDPE/POF composites increased the impact energy compared to HDPE/POF composites without a coupling agent. Thus, the fiber could absorb energy because of strong fiber–matrix interfacial adhesion.

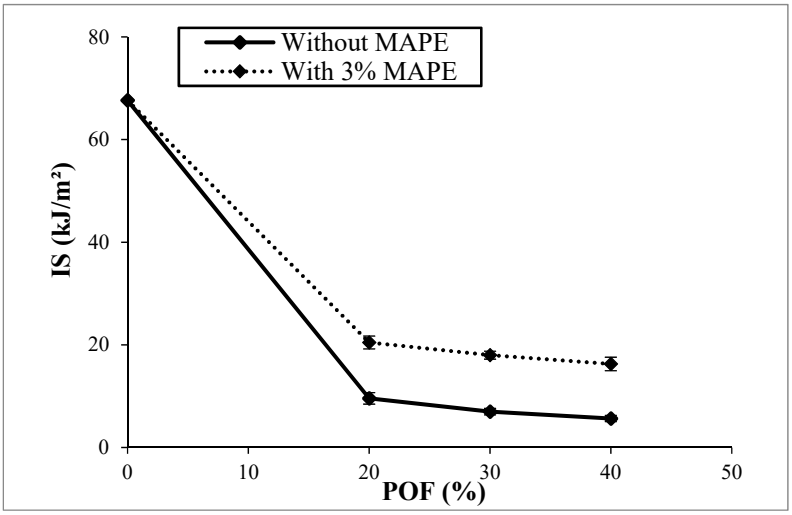

Figure 7. Effect of the POF content on impact strength (IS) of the HDPE/POF composites (with and without 3% MAPE).

3.4. Torque Rheology

Torque rheology is used to determine the processing parameters of the composite blends. Black spruce wood fiber (WFBS) is also incorporated into the HDPE matrix to evaluate the influence of different lignocellulosic reinforcing agents on the torque rheological properties. Figure 8 shows the torque versus mixing time curves of HDPE reinforced

with POF and WFBS at 20, 30, and 40 wt% (without MAPE) obtained at 170 °C in a torque rheometer. For all the composite materials, the torque reaches a stable state of approximately 8–10 min and remains constant until the end of the 12 min compounding period. This observation suggests successful mixing without material degradation. Figure 8a,b show that the processing torque was affected by both the fiber ratio and type. From the curves depicted in Figure 8, we can determine the stabilized torque (after 12 min of mixing) and calculate the mechanical energy (E_m) (Equation (2)):

$$E_m = 2\pi \times N \int_1^2 M \, dt \quad (2)$$

N is 50 RPM and M is the torque (Nm).

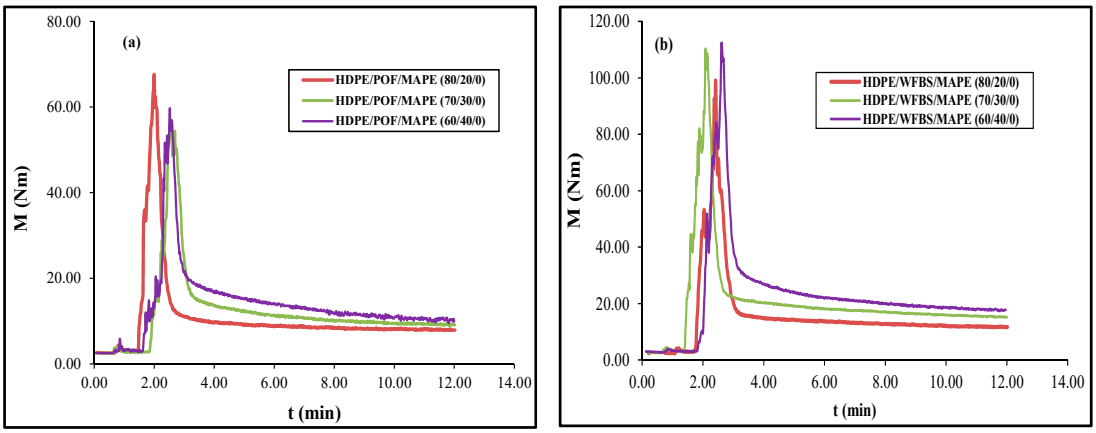

Figure 8. Effect of fiber content and mixing time at 170 °C and 50 RPM on the torque of (**a**) HDPE/POF and (**b**) HDPE/WFBS composites (without coupling agent).

Figure 9 illustrates the effect of fiber content on the stabilized torque and E_m of HDPEPOF and WFBS composites (without MAPE). From these results, we can conclude that the stabilized torque (or balancing torque) and E_m of HDPE/POF and HDPE/WFBS composites increase with increasing fiber content (POF and WFBS) (Figure 9a,b). Higher fiber load led to increasing torque and, consequently, greater energy. Saddem et al. [61] observed a similar trend for wood–plastic composites. An increase in fiber load enhances fiber–fiber interactions and reduces the fiber wettability by the polymeric matrix [61–63]. Furthermore, the HDPE/WFBS composites give greater values of the maximum and stabilized torque than the HDPE/POF composites (Figures 8 and 9a). The difference in chemical composition between WFBS and POF explains this result. WFBS showed higher lignin (31.9%) and hot water extractive (12.7%) contents [64] than the POF, which has 29.3% and 6.72% lignin and hot water extractive contents, respectively [25]. Saddem et al. [61] reported similar findings. They concluded that higher lignin content in jack pine bark fibers leads to increased torque and poor fiber dispersion within the composite, consequently reducing its mechanical properties. Also, the viscosity of the fiber/polymer blend is significantly influenced by the fiber volume fraction, which in turn depends on the fiber density.

A lower fiber density corresponds to a higher fraction volume, contributing to an elevated viscosity and torque mixture [61]. In this context, the WFBS shows a lower density value (0.639 g/cm^3 [64]) than the density value of the POF (1.214 g/cm^3 [65]), which explains the greater values of the maximum and stabilized torque of the HDPE/WFBS composites compared to HDPE/POF composites.

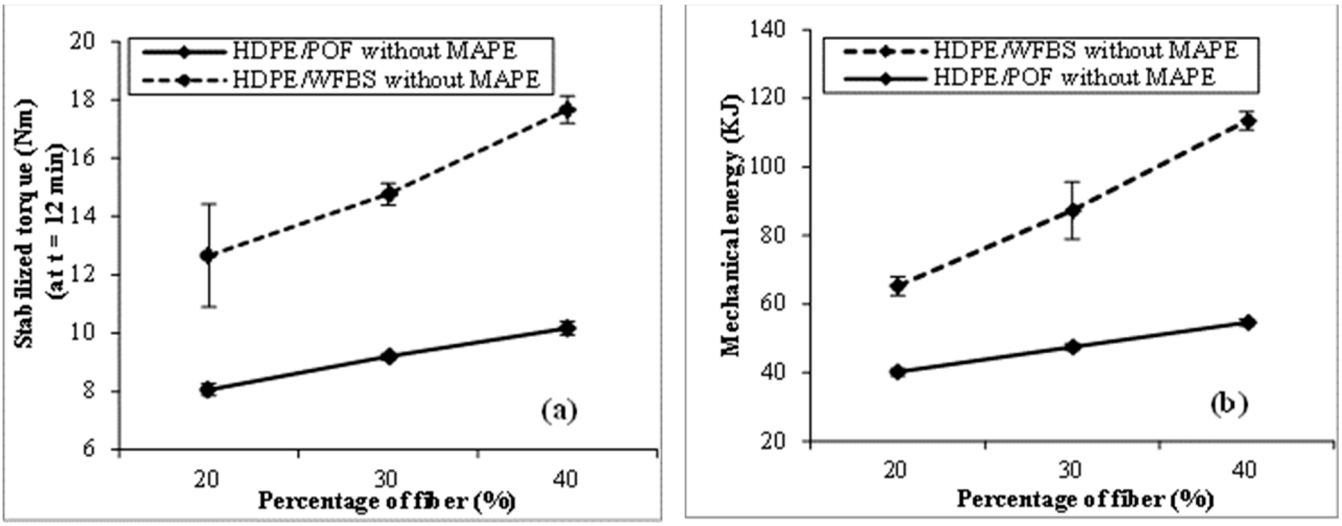

Figure 9. Effect of fiber content (POF and WFBS) on stabilized torque (**a**) and mechanical energy (**b**) for HDPE/POF and HDPE/WFB composites without MAPE.

Figure 10 depicts the influence of the MAPE on the stabilized torque and E_m of the HDPE/WFBS and HDPE/POF composites reinforced with 40 wt% fibers. Adding MAPE increases the stabilized torque and E_m for HDPE/WFBS of the composites compared with those without MAPE (See Figure 10a,b). The better adhesion between the fiber and matrix with the addition of MAPE explains this result. Similar findings were observed by Li et al. [66], who reported that the addition of MAPE (lower than 5 wt%) enhanced the equilibrium torque of the HDPE/Wood (40/60) composites, compared with the composites without MAPE.

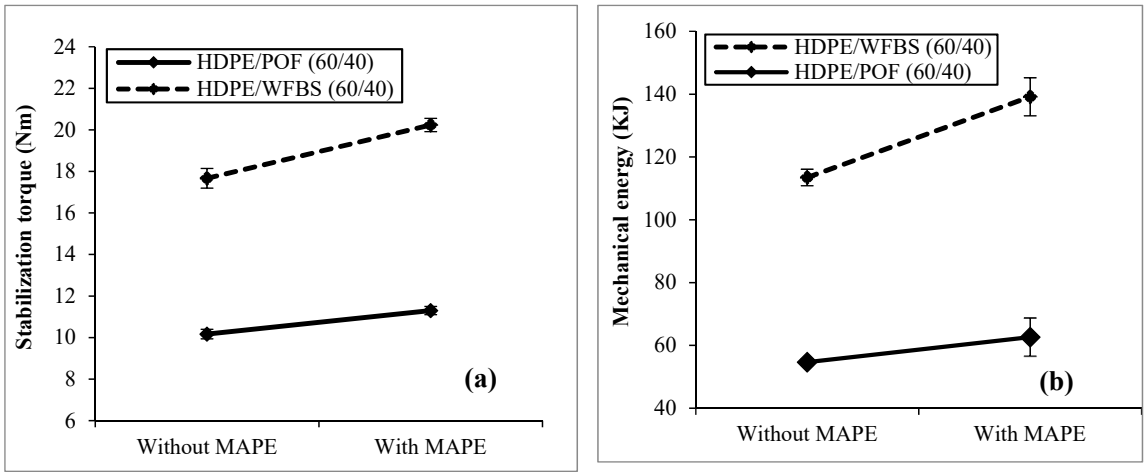

Figure 10. Effect of 3% MAPE on (**a**) stabilized torque and (**b**) mechanical energy (**b**) for composites (HDPE/POF and HDPE/WFB) reinforced with 40 wt% fiber.

4. Conclusions

This study investigated the properties of HDPE reinforced with POF and coupled with 3 wt% MAPE. The latter reduced the hydrophilic characteristics of the lignocellulosic fiber. Results indicate that increasing the POF content enhanced the composite stiffness, crystallinity, and torque rheological properties. The coupling agent improved the interfacial adhesion between POF and HDPE and the composites' tensile properties, ductility, and crystallinity. The HDPE/POF/MAPE composites have potential as an alternative to conventional materials, especially for building applications.

Author Contributions: Conceptualization, M.H. and A.E.; methodology, M.H., software, A.K.; validation, A.E., A.K. and C.B.; formal analysis, M.H.; investigation, M.H.; resources, A.K. and C.B.; data curation, M.H.; writing—original draft preparation, M.H.; writing—review and editing, A.E., A.K. and C.B.; visualization, M.H.; supervision, A.E., A.K. and C.B.; project administration, A.E., A.K. and C.B.; funding acquisition, A.K. and C.B. All authors have read and agreed to the published version of the manuscript.

Funding: The Tunisian Ministry of Higher Education and Scientific Research, the Canada Research Chairs Program Fund number: 592380, and the Natural Sciences and Engineering Research Council of Canada (NSERC), Fund Number: 567663 supported this study.

Data Availability Statement: Data will be available upon request.

Acknowledgments: The authors thank Williams Belhadef for technical support and Sebastien Migneault for scientific guidance.

Conflicts of Interest: The authors declare no conflicts of interest.

References

1. Boukettaya, S.; Alawar, A.; Almaskari, F.; Ben Daly, H.; Abdala, A.; Chatti, S. Modeling of water diffusion mechanism in polypropylene/date palm fiber composite materials. *J. Compos. Mater.* **2018**, *52*, 2651–2659. [CrossRef]
2. El Abbassi, F.E.; Assarar, M.; Ayad, R.; Sabhi, H.; Buet, S.; Lamdouar, N. Effect of recycling cycles on the mechanical and damping properties of short alfa fibre reinforced polypropylene composite. *J. Renew. Mater.* **2019**, *7*, 253. [CrossRef]
3. Haddar, M.; Ben Slim, Y.; Koubaa, S. Mechanical and water absorption behavior of thermoset matrices reinforced with natural fiber. *Polym. Compos.* **2022**, *43*, 3481–3495. [CrossRef]
4. Zhao, X.; Copenhaver, K.; Wang, L.; Korey, M.; Gardner, D.J.; Li, K.; Lamm, M.E.; Kishore, V.; Bhagia, S.; Tajvidi, M.; et al. Recycling of natural fiber composites: Challenges and opportunities. *Resour. Conserv. Recy.* **2022**, *177*, 105962. [CrossRef]
5. Rangappa, S.M.; Siengchin, S.; Parameswaranpillai, J.; Jawaid, M.; Ozbakkaloglu, T. Lignocellulosic fiber reinforced composites: Progress, performance, properties, applications, and future perspectives. *Polym. Compos.* **2022**, *43*, 645–691. [CrossRef]
6. Naik, N.; Sooriyaperakasam, N.; Abeykoon, Y.K.; Wijayarathna, Y.S.; Pranesh, G.; Roy, S.; Negi, R.; Aakif, B.K.; Kulatungag, A.; Kandasamy, J. Sustainable Green Composites: A Review of Mechanical Characterization, Morphological Studies, Chemical Treatments and their Processing Methods. *J. Comput. Mech. Manag.* **2022**, *1*, 66–81. [CrossRef]
7. Chandrasekar, M.; Shahroze, R.M.; Ishak, M.R.; Saba, N.; Jawaid, M.; Senthilkumar, K.; Kumar, T.S.M.; Siengchin, S. Flax and sugar palm reinforced epoxy composites: Effect of hybridization on physical, mechanical, morphological and dynamic mechanical properties. *Mater. Res. Express* **2019**, *6*, 105331. [CrossRef]
8. More, A.P. Flax fiber–based polymer composites: A review. *Adv. Compos. Hybrid. Mater.* **2022**, *5*, 1–20. [CrossRef]
9. Asyraf, M.R.M.; Rafidah, M.; Azrina, A.; Razman, M.R. Dynamic mechanical behaviour of kenaf cellulosic fibre biocomposites: A comprehensive review on chemical treatments. *Cellulose* **2021**, *28*, 2675–2695. [CrossRef]
10. Messaoui, S.; Borchani, K.E.; Ghali, L.; Guermazi, N.; Haddar, N.; Msahli, S. Effect of a New Composition Ratio and of a New Chemical Treatment on Natural Alfa Fiber/polypropylene Composites Manufacturing and Their Mechanical Properties. *J. Nat. Fibers* **2022**, *19*, 10126–10141. [CrossRef]
11. Mousavi, S.R.; Zamani, M.H.; Estaji, S.; Tayouri, M.I.; Arjmand, M.; Jafari, S.H.; Nouranian, S.; Khonakdar, H.A. Mechanical properties of bamboo fiber-reinforced polymer composites: A review of recent case studies. *J. Mater. Sci.* **2022**, *57*, 3143–3167. [CrossRef]
12. Radzi, A.M.; Zaki, S.A.; Hassan, M.Z.; Ilyas, R.A.; Jamaludin, K.R.; Daud, M.Y.M.; Aziz, S.A.A. Bamboo-Fiber-Reinforced thermoset and thermoplastic polymer composites: A review of properties, fabrication, and potential applications. *Polymers* **2022**, *14*, 1387. [CrossRef] [PubMed]
13. Asyraf, M.R.M.; Ishak, M.R.; Syamsir, A.; Nurazzi, N.M.; Sabaruddin, F.A.; Shazleen, S.S.; Norrrahim, M.N.F.; Rafidah, M.; Ilyas, R.A.; Rashid, M.Z.A.; et al. Mechanical properties of oil palm fibre-reinforced polymer composites: A review. *J. Mater. Res. Technol.* **2022**, *17*, 33–65. [CrossRef]
14. Asyraf, M.R.M.; Ishak, M.R.; Norrrahim, M.N.F.; Nurazzi, N.M.; Shazleen, S.S.; Ilyas, R.A.; Rafidah, M.; Razman, M.R. Recent advances of thermal properties of sugar palm lignocellulosic fibre reinforced polymer composites. *Int. J. Biol. Macromol.* **2021**, *193*, 1587–1599. [CrossRef] [PubMed]
15. Asyraf, M.R.M.; Rafidah, M.; Ebadi, S.; Azrina, A.; Razman, M.R. Mechanical properties of sugar palm lignocellulosic fibre reinforced polymer composites: A review. *Cellulose* **2022**, *29*, 6493–6516. [CrossRef]
16. Asyraf, M.R.M.; Syamsir, A.; Supian, A.B.M.; Usman, F.; Ilyas, R.A.; Nurazzi, N.M.; Norrrahim, M.N.F.; Razman, M.R.; Zakaria, S.Z.S.; Sharma, S.; et al. Sugar palm fibre-reinforced polymer composites: Influence of chemical treatments on its mechanical properties. *Materials* **2022**, *15*, 3852. [CrossRef] [PubMed]
17. Chandekar, H.; Chaudhari, V.; Waigaonkar, S. A review of jute fiber reinforced polymer composites. *Mater. Today Proc.* **2020**, *6*, 2079–2082. [CrossRef]

18. Sahoo, G.; Kamalakannan, R.; Pradeep, G.M.; Manivelmuralidaran, V.; Girimurugan, R. A process of analyzing the performance evaluation of sisal fiber in fiber reinforced composites. *Mater. Today Proc.* **2022**, *56*, 3201–3206. [CrossRef]
19. Stelea, L.; Filip, I.; Lisa, G.; Ichim, M.; Drobotă, M.; Sava, C.; Mureșan, A. Characterisation of hemp fibres reinforced composites using thermoplastic polymers as matrices. *Polymers* **2022**, *14*, 481. [CrossRef]
20. Holbery, J.; Houston, D. Natural-fiber-reinforced polymer composites in automotive applications. *Jom* **2006**, *58*, 80–86. [CrossRef]
21. Mastura, M.T.; Sapuan, S.M.; Mansor, M.R.; Nuraini, A.A. Materials selection of thermoplastic matrices for 'green' natural fibre composites for automotive anti-roll bar with particular emphasis on the environment. *Int. J. Precis. Eng. Manuf.-Green Technol.* **2018**, *5*, 111–119. [CrossRef]
22. Jaafar, J.; Siregar, J.P.; Salleh, S.M.; Hamdan, M.M.H.; Cionita, T.; Rihayat, T. Important considerations in manufacturing of natural fiber composites: A review. *Int. J. Precis. Eng. Manuf.-Green Technol.* **2019**, *6*, 647–664. [CrossRef]
23. Mohammed, L.; Ansari, M.N.M.; Pua, G.; Jawaid, M.; Islam, M.S. A Review on Natural Fiber Reinforced Polymer Composite and Its Applications. *Int. J. Polym. Sci.* **2015**, *2015*, 243947. [CrossRef]
24. Valášek, P.; Ruggiero, A.; Müller, M. Experimental description of strength and tribological characteristic of EFB oil palm fibres/epoxy composites with technologically undemanding preparation. *Compos. Part B Eng.* **2017**, *122*, 79–88. [CrossRef]
25. Haddar, M.; Elloumi, A.; Koubaa, A.; Bradai, C.; Migneault, S.; Elhalouani, F. Synergetic effect of *Posidonia oceanica* fibers and deinking paper sludge on the thermo-mechanical properties of high-density polyethylene composites. *Ind. Crops Prod.* **2018**, *121*, 26–35. [CrossRef]
26. Kim, J.W.; Lee, D.G. Study on the fiber orientation during compression molding of reinforced thermoplastic composites. *Int. J. Precis. Eng. Manuf.-Green. Tech.* **2014**, *1*, 335–339. [CrossRef]
27. Haddar, M.; Koubaa, S.; Issaoui, M.; Frikha, A. Optimization in the reprocessing of recycled polyamide 6 reinforced with 30 wt% Glass Fiber (PA6/GF30) using mixture design. *Polym. Adv. Technol.* **2024**, *35*, e6240. [CrossRef]
28. Correa-Aguirre, J.P.; Luna-Vera, F.; Caicedo, C.; Vera-Mondragón, B.; Hidalgo-Salazar, M.A. The effects of reprocessing and fiber treatments on the properties of polypropylene-sugarcane bagasse biocomposites. *Polymers* **2020**, *12*, 1440. [CrossRef] [PubMed]
29. Latif, R.; Wakeel, S.; Khan, N.Z.; Siddiquee, A.N.; Verma, S.L.; Khan, Z.A. Surface treatments of plant fibers and their effects on mechanical properties of fiber-reinforced composites: A review. *J. Reinf. Plast. Compos.* **2019**, *38*, 15–30. [CrossRef]
30. Shekar, H.S.; Ramachandra, M. Green Composites: A Review. *Mater. Today Proc.* **2018**, *5*, 2518–2526. [CrossRef]
31. Zainal, M.; Santiagoo, R.; Ayob, A.; Ghani, A.A.; Mustafa, W.A.; Othman, N.S. Thermal and mechanical properties of chemical modification on sugarcane bagasse mixed with polypropylene and recycle acrylonitrile butadiene rubber composite. *J. Thermoplast. Compos. Mater.* **2020**, *33*, 1533–1554. [CrossRef]
32. Madhavi, S.; Raju, N.V.; Johns, J. Characterization of bamboo-polypropylene composites: Effect of coupling agent. *Fibers Polym.* **2021**, *22*, 3183–3191. [CrossRef]
33. Li, Y. Effect of coupling agent concentration, fiber content, and size on mechanical properties of wood/HDPE composites. *Int. J. Polym. Mater. Polym. Biomater.* **2012**, *61*, 882–890. [CrossRef]
34. Hachaichi, A.; Nekkaa, S.; Amroune, S.; Jawaid, M.; Alothman, O.Y.; Dufresne, A. Effect of alkali surface treatment and compatibilizer agent on tensile and morphological properties of date palm fibers-based high-density polyethylene biocomposites. *Polym. Compos.* **2022**, *43*, 7211–7221. [CrossRef]
35. Bouafif, H.; Koubaa, A.; Perré, P.; Cloutier, A.; Riedl, B. Wood particle/high-density polyethylene composites: Thermal sensitivity and nucleating ability of wood particles. *J. Appl. Polym. Sci.* **2009**, *113*, 593–600. [CrossRef]
36. Wunderlich, B. *Macromolecular Physics II*; Academic Press: New York, NY, USA, 1973.
37. *ASTM D638*; Standard Test Method for Tensile Properties of Plastics. ASTM International: West Conshohocken, PA, USA, 2003; p. 15.
38. *ASTM D4812*; Standard Test Method for Unnotched Cantilever Beam Impact Resistance of Plastics. ASTM International: West Conshohocken, PA, USA, 1999; p. 11.
39. Araujo, J.R.; Mano, B.; Teixeira, G.M.; Spinacé, M.A.S.; De Paoli, M.A. Biomicrofibrilar composites of high-density polyethylene reinforced with curaua fibers: Mechanical, interfacial and morphological properties. *Compos. Sci. Tech.* **2010**, *70*, 1637–1644. [CrossRef]
40. Haddar, M.; Elloumi, A.; Koubaa, A.; Bradai, C.; Migneault, S.; Elhalouani, F. Effect of high content of deinking paper sludge (DPS) on the reinforcement of HDPE. *J. Polym. Environ.* **2017**, *25*, 617–627. [CrossRef]
41. Kaci, M.; Hamma, A.; Pillin, I.; Grohens, Y. Effect of reprocessing cycles on the morphology and properties of poly(propylene)/wood flour composites compatibilized with EBAGMA terpolymer. *Macromol. Mater. Eng.* **2009**, *294*, 532–540. [CrossRef]
42. Essabir, H.; Boujmal, R.; Bensalah, M.O.; Rodrigue, D.; Bouhfid, R.; Qaiss, A.E.K. Mechanical and thermal properties of hybrid composites: Oil-palm fiber/clay reinforced high-density polyethylene. *Mech. Mater.* **2016**, *98*, 36–43. [CrossRef]
43. Balasuriya, P.W.; Ye, L.; Mai, Y.W.; Wu, J. Mechanical properties of wood flake-polyethylene composites. II. Interface modification. *J. Appl. Poly. Sci.* **2002**, *83*, 2505–2521. [CrossRef]
44. Părpăriţă, E.; Darie, R.N.; Popescu, C.M.; Uddin, M.A.; Vasile, C. Structure-morphology-mechanical properties relationship of some polypropylene/lignocellulosic composites. *Mater. Des.* **2014**, *56*, 763–772. [CrossRef]
45. Lisperguer, J.; Perez, P.; Urizar, S. Structure and thermal properties of lignins: Characterization by infrared spectroscopy and differential scanning calorimetry. *J. Chil. Chem. Soc.* **2009**, *54*, 460–463. [CrossRef]

46. Robledo-Ortíz, J.R.; González-López, M.E.; Rodrigue, D.; Gutiérrez-Ruiz, J.F.; Prezas-Lara, F.; Pérez-Fonseca, A.A. Improving the compatibility and mechanical properties of natural fibers/green polyethylene biocomposites produced by rotational molding. *J. Polym. Environ.* **2020**, *28*, 1040–1049. [CrossRef]
47. Mulinari, D.R.; Voorwald, H.J.; Cioffi, M.O.; da Silva, M.L. Cellulose fiber-reinforced high-density polyethylene composites—Mechanical and thermal properties. *J. Compos. Mater.* **2017**, *51*, 1807–1815. [CrossRef]
48. Tazi, M.; Erchiqui, F.; Godard, F.; Kaddami, H.; Ajji, A. Characterization of rheological and thermophysical properties of HDPE-wood composite. *J. Appl. Polym. Sci.* **2014**, *131*, 40495–40506. [CrossRef]
49. Mulinari, D.R.; Guedes, J.R.; Simba, B.G. Low-density polyethylene composites reinforced with Australian King Palm fibers: Mechanical and thermal properties. *Polym. Bull.* **2017**, *74*, 4549–4559. [CrossRef]
50. Torres-Tello, E.V.; Robledo-Ortíz, J.R.; González-García, Y.; Pérez-Fonseca, A.A.; Jasso-Gastinel, C.F.; Mendizábal, E. Effect of agave fiber content in the thermal and mechanical properties of green composites based on polyhydroxybutyrate or poly (hydroxybutyrate-co-hydroxyvalerate). *Ind. Crops Prod.* **2017**, *99*, 117–125. [CrossRef]
51. Roumeli, E.; Terzopoulou, Z.; Pavlidou, E.; Chrissafis, K.; Papadopoulou, E.; Athanasiadou, E.; Triantafyllidis, K.; Bikiaris, D.N. Effect of maleic anhydride on the mechanical and thermal properties of hemp/high-density polyethylene green composites. *J. Therm. Anal. Calorim.* **2015**, *121*, 93–105. [CrossRef]
52. Yang, H.S.; Wolcott, M.P.; Kim, H.S.; Kim, H.J. Thermal properties of lignocellulosic filler-thermoplastic polymer bio-composites. *J. Therm. Anal. Calorim.* **2005**, *82*, 157–160. [CrossRef]
53. Ferrero, B.; Fombuena, V.; Fenollar, O.; Boronat, T.; Balart, R. Development of natural fiber-reinforced plastics (NFRP) based on biobased polyethylene and waste fibers from *Posidonia oceanica* seaweed. *Polym. Compos.* **2015**, *36*, 1378–1385. [CrossRef]
54. Borja, Y.; Rieß, G.; Lederer, K. Synthesis and characterization of polypropylene reinforced with cellulose I and II fibers. *J. Appl. Polym. Sci.* **2006**, *101*, 364–369. [CrossRef]
55. Joseph, P.V.; Joseph, K.; Thomas, S.; Pillai, C.K.S.; Prasad, V.S.; Groeninckx, G.; Sarkissova, M. The thermal and crystallisation studies of short sisal fibre reinforced polypropylene composites. *Compos. Part A Appl. Sci. Manuf.* **2003**, *34*, 253–266. [CrossRef]
56. Bendahou, A.; Kaddami, H.; Sautereau, H.; Raihane, M.; Erchiqui, F.; Dufresne, A. Short palm tree fibers polyolefin composites: Effect of filler content and coupling agent on physical properties. *Macromol. Mater. Eng.* **2008**, *293*, 140–148. [CrossRef]
57. Khiari, R.; Marrakchi, Z.; Belgacem, M.N.; Mauret, E.; Mhenni, F. New lignocellulosic fiber-reinforced composite materials: A stepforward in the valorization of the *Posidonia oceanica* balls. *Compos. Sci. Technol.* **2011**, *71*, 1867–1872. [CrossRef]
58. Puglia, D.; Petrucci, R.; Fortunati, E.; Luzi, F.; Kenny, J.M.; Torre, L. Revalorisation of *Posidonia oceanica* as reinforcement in polyethylene/maleic anhydride grafted polyethylene composites. *J. Renew. Mater.* **2014**, *2*, 66–76. [CrossRef]
59. Ndiaye, D.; Tidjani, A. Effects of coupling agents on thermal behavior and mechanical properties of wood flour/polypropylene composites. *J. Compos. Mater.* **2012**, *46*, 3067–3075. [CrossRef]
60. Naghmouchi, I.; Espinach, F.X.; Mutjé, P.; Boufi, S. Polypropylene composites based on lignocellulosic fillers: How the filler morphology affects the composite properties. *Mater. Des.* **2015**, *65*, 454–461. [CrossRef]
61. Saddem, M.; Koubaa, A.; Bouafif, H.; Migneault, S.; Riedl, B. Effect of fiber and polymer variability on the rheological properties of wood polymer composites during processing. *Polym. Compos.* **2019**, *40*, 609–616. [CrossRef]
62. Teuber, L.; Militz, H.; Krause, A. Processing of wood plastic composites: The influence of feeding method and polymer melt flow rate on particle degradation. *J. Appl. Polym. Sci.* **2016**, *133*, 43231. [CrossRef]
63. Zhang, J.; Koubaa, A.; Xing, D.; Liu, W.; Wang, H.; Wang, X.; Wang, Q. High-performance lignocellulose/polycarbonate biocomposites fabricated by in situ reaction: Structure and properties. *Compos. Part A Appl. Sci. Manuf.* **2020**, *138*, 106068. [CrossRef]
64. Yemele, M.C.N.; Koubaa, A.; Cloutier, A.; Souloungange, P.; Wolcott, M. Effect of bark fiber content and size on the mechanical properties of bark/HDPE composites. *Compos. Part A Appl. Sci. Manuf.* **2010**, *41*, 131–137. [CrossRef]
65. Hamdaoui, O.; Limam, O.; Ibos, L.; Mazioud, A. Thermal and mechanical properties of hardened cement paste reinforced with Posidonia-Oceanica natural fibers. *Constr. Build. Mater.* **2021**, *269*, 121339. [CrossRef]
66. Li, X.; Tabil, L.G.; Panigrahi, S. Chemical treatments of natural fiber for use in natural fiber-reinforced composites: A review. *J. Polym. Environ.* **2007**, *15*, 25–33. [CrossRef]